ORIGINAL PAPER

# Theoretical study of the reaction of CH₂XO (X = F, Cl, Br) radicals with the NO radical

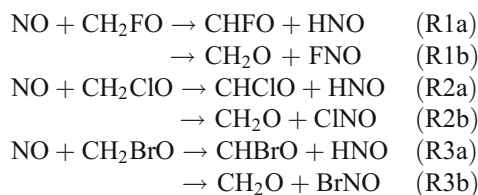Yue Li · Hui Zhang · Qingguo Chen · Zesheng Li

**Abstract** In this paper, we focus on the multiple-channel reactions of CH₂XO (X = F, Cl, Br) radicals with the NO radical by means of direct dynamic methods. All structures of the stationary points were obtained at the MP2/6-311+G(d,p) level and vibrational frequency analysis was also performed at this level of theory. The minimum energy path (MEP) was obtained via the intrinsic reaction coordinate (IRC) theory at the MP2/6-311+G(d,p) level, and higher-level energetic information was refined by the MC-QCISD method. The rate constants for the three hydrogen abstraction reaction channels over the temperature range 200–1,500 K were calculated by the improved canonical variational transition state theory (ICVT) with a correction for small-curvature tunneling (SCT). The rate constants calculated in this manner were in good agreement with the available experimental data, and the three-parameter rate–temperature formulae for the temperature range 200–1,500 K were $k_{1a}(T) = 0.32 \times 10^{-18} T^{1.83} \exp(1748.54/T)$, $k_{2a}(T) = 0.22 \times 10^{-19} T^{2.19} \exp(1770.19/T)$, $k_{3a}(T) = 0.88 \times 10^{-20} T^{2.20} \exp(1513.82/T)$ (in units of cm³ molecule⁻¹ s⁻¹).

**Keywords** Gas-phase reaction · Transition state · Rate constants

Y. Li · H. Zhang (✉)
College of Chemical and Environmental Engineering,
Harbin University of Science and Technology, Harbin 150080,
People's Republic of China
e-mail: hust_zhanghui11@hotmail.com

Q. Chen (✉)
College of Electrical and Electronic Engineering, Harbin
University of Science and Technology, Harbin 150080,
People's Republic of China
e-mail: qgchen@263.net

Z. Li (✉)
Academy of Fundamental and Interdisciplinary Sciences,
Department of Chemistry, Harbin Institute of Technology,
Harbin 150080, People's Republic of China
e-mail: zeshengli@bit.edu.cn

Z. Li
Key Laboratory of Cluster Science of Ministry of Education
& School of Chemistry, Beijing Institute of Technology,
Beijing 100081, People's Republic of China

## Introduction

Halogen-containing compounds are important products of the incineration of municipal waste [1], as well as significant atmospheric pollutants. Halogen-substituted alkoxy radicals are known to be important intermediates in the combustion of halogen-containing compounds [2–4]. In the atmosphere, a halogen-substituted alkoxy radical CH₂XO (X = F, Cl, Br) can react with an NO radical, leading to the abstraction of either an H atom or the halogen atom from the CH₂XO (X = F, Cl, Br) radical. We therefore have six feasible reaction pathways for the title reaction (denoted R1a, R1b, R2a, R2b, R3a, R3b, respectively), as follows:

$$NO + CH_2FO \rightarrow CHFO + HNO \quad (R1a)$$
$$\rightarrow CH_2O + FNO \quad (R1b)$$
$$NO + CH_2ClO \rightarrow CHClO + HNO \quad (R2a)$$
$$\rightarrow CH_2O + ClNO \quad (R2b)$$
$$NO + CH_2BrO \rightarrow CHBrO + HNO \quad (R3a)$$
$$\rightarrow CH_2O + BrNO \quad (R3b)$$

In 2001, F. X. Wu and R. W. Carr [3] obtained the rate constants for the reaction NO + CH₂ClO → CHClO + HNO (R2a) over the temperature range 265–306 K by UV flash photolysis with time-resolved mass spectrometry. The experimental value at 289 K was $(2.70 \pm 0.4) \times 10^{-12}$ cm³ molecule⁻¹ s⁻¹.

For the title reactions, experimental measurements were performed in the low-temperature range, and no experimental data are available for the high-temperature range. However, the rate constant must be evaluated at high temperatures if we are to gain a deeper understanding of the mechanism of this multiple-channel reaction. Consequently, it is necessary to calculate the rate constant at high temperatures theoretically. To the best of our knowledge, no previous theoretical work on the kinetics of the title reactions has been reported.

In the work described in this paper, the kinetics of the reactions of $CH_2XO$ (X = F, Cl, Br) radicals with the NO radical were studied using a dual-level direct dynamics method [5–9]. The potential energy surface information (geometries, energies, gradients, force constants) of all the stationary points (reactants, complexes, products, and transition states) and 16 points (eight points in the reactant channel, eight points in the product channel) selected along the minimum energy path (MEP) of each reaction channel were obtained directly from electronic structure calculations at the MP2/6-311+G(d,p) level. Complex energies corrected for basis set superposition error (BSSE) were further confirmed by the standard counterpoise method of Boys and Bernardi [10]. Higher-level single-point energy corrections were performed by the MC-QCISD method [11]. Subsequently, the POLYRATE 9.7 program [12] was employed to calculate the rate constants of the three hydrogen abstraction reaction channels by the variational transition state theory (VTST) [13, 14] proposed by Truhlar and coworkers. Theoretical and experimental results were then compared. Our results may prove useful in further experimental investigations.

## Computational methods

In the present work, we optimized the equilibrium geometries and vibrational frequencies of all of the stationary points (reactants, complexes, products, and transition states) at the restricted or unrestricted second-order Møller–Plesset perturbation (MP2) [15–18] level with the 6-311+G(d,p) basis set. Complex energies were further confirmed with BSSE correction. Using intrinsic reaction coordinate (IRC) theory, the MEP was obtained with a gradient step size of $0.05 \ (amu)^{1/2}$ bohr at the MP2/6-311+G(d,p) level. The first and second derivatives of the energy were then obtained to calculate the curvature of the reaction path and the generalized vibrational frequencies along the reaction path. The MC-QCISD method (multi-coefficient correlation method based on quadratic configuration interaction with single and double excitations, proposed by Fast and Truhlar) [11] was employed to refine the energy information in order to get more accurate energies and barrier heights, based on the MP2/6-311+G(d,p) geometries. All of the calculations were performed using the GAUSSIAN 03 software package [19].

VTST [13, 14] was used to calculate the rate constants in the program POLYRATE 9.7 [12]. The theoretical rate constants for the three hydrogen abstraction reaction channels over the temperature range 200–1,500 K were calculated using the improved canonical variational transition state theory (ICVT) [20] with the small-curvature tunneling (SCT) [21] correction proposed by Truhlar and coworkers [20]. For the three reaction channels, all of the vibrational modes were treated as separable quantum harmonic oscillators. The curvature components were calculated using a quadratic fit to obtain the derivative of the gradient with respect to the reaction coordinate.

## Results and discussions

### Stationary points

The optimized structures of the reactants ($CH_2FO$, $CH_2ClO$, $CH_2BrO$, and NO), complexes (CR1a, CR2a, and CR3a), products (CHFO, CHClO, CHBrO, HNO, FNO, ClNO, BrNO, and $CH_2O$), and transition states (TS1a, TS1b, TS2a, TS2b, TS3a, and TS3b) calculated at the MP2/6-311+G(d,p) level are depicted in Fig. 1, along with the available experimental values [22, 23]. The theoretical geometric parameters of NO, HNO, CHFO, $CH_2O$, FNO, and ClNO are in good agreement with the corresponding experimental values [22, 23]. In Fig. 1, all of the transition states have the same symmetry, $C_1$. In the structures TS1a, TS2a, and TS3a, the C—H bond that breaks is elongated by 23 %, 23 %, and 26 % compared to the equilibrium bond lengths in $CH_2FO$, $CH_2ClO$, and $CH_2BrO$, respectively; the resulting N—H bond is stretched by 33 %, 30 %, and 31 % compared to the equilibrium bond length in isolated HNO, respectively. Thus, the elongation of the breaking C—H bond is smaller than the elongation of the resulting N—H bond. Similarly, for the structures TS1b, TS2b, and TS3b, the breaking bonds are again less elongated than the resulting bonds, indicating that the abovementioned reaction channels are all reactant-like (i.e., the six reaction channels proceed via "early" transition states, which is consistent with Hammond's postulate [24] for an exothermic reaction).

The harmonic vibrational frequencies of the stationary points (including the reactants, complexes, products, and transition states) obtained at the MP2/6-311+G(d,p) level as well as the experimental values available [25–27] are presented in Table 1. It is obvious that the calculated frequencies for the species HNO, CHClO, and $CH_2O$ are in agreement with their corresponding experimental values, with the largest deviation being <9 %. The six transition states were all confirmed by normal-mode analysis as having one and only one imaginary frequency, which corresponds to the stretching mode for coupling between the breaking and forming bonds.
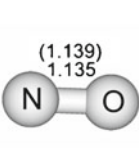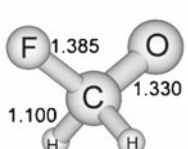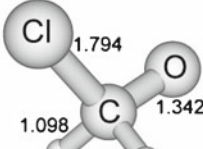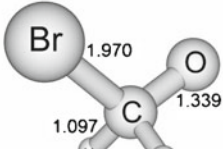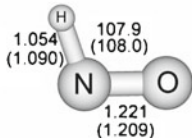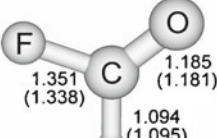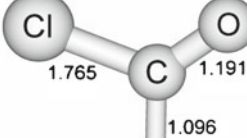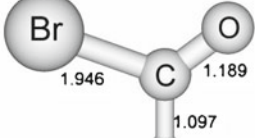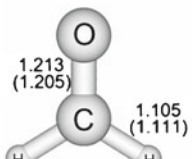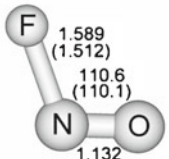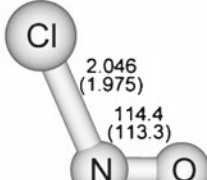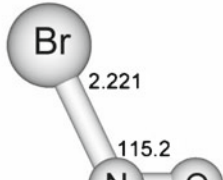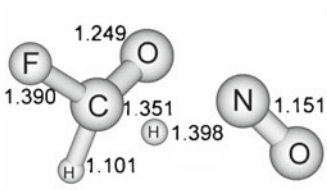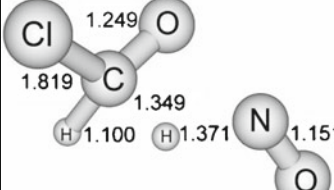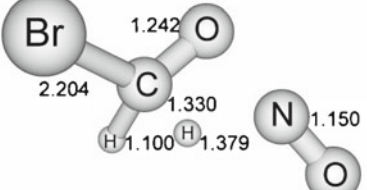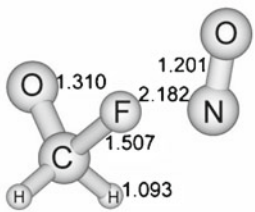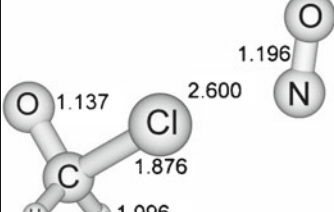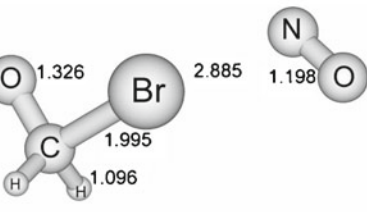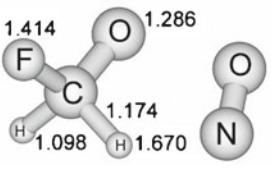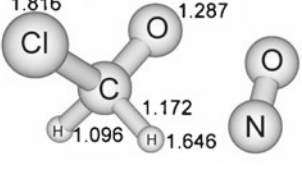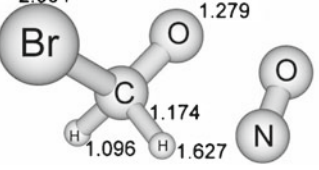
**Fig. 1** Optimized geometries of the reactants, products, complexes, and transition states calculated at the MP2/6-311+G(d,p) level. The *values in parentheses* are the experimental values (obtained from [22, 23] for NO, HNO, CHFO, FNO, ClNO, and CH₂O, respectively). Bond lengths are in angstroms and angles are in degrees

**Table 1** Calculated and experimental frequencies (in cm$^{-1}$) for the reactants, complexes, products, and transition states for the title reactions, calculated at the MP2/6-311+G(d,p) level

| Species | Value(s) calculated via MP2/6-311+G(d,p) | Experimentally determined values |
|---|---|---|
| NO | 3553 | |
| CH$_2$FO | 3090, 3028, 1425, 1411, 1212, 1143, 1035, 845, 556 | |
| CH$_2$ClO | 3049, 3110, 1381, 1368, 1121, 1111, 750, 710, 415 | |
| CH$_2$BrO | 3118, 3052, 1383, 1309, 1111, 1050, 641, 631, 335 | |
| HNO | 3035, 1582, 1500 | 2756, 1563,1511[a] |
| CHFO | 3166, 1860, 1397, 1063, 1043, 662 | |
| CHClO | 3112, 1793, 1386, 970, 769, 473 | 2929, 1784, 1307, 932, 739, 457[b] |
| CHBrO | 3098, 1795, 1344, 926, 661, 369 | |
| CH$_2$O | 3049, 2977, 1762, 1558, 1278, 1205 | 2843, 2782, 1746, 1500, 1249, 1167[c] |
| FNO | 1937, 712, 441 | |
| ClNO | 1892, 579, 313 | |
| BrNO | 1896, 531, 261 | |
| CR1a | 3077, 2285, 1899, 1509, 1380, 1315, 1263, 1020, 935, 641, 553, 401, 373, 248, 126 | |
| CR2a | 3091, 2303, 1899, 1498, 1334, 1287, 1236, 938, 683, 622, 423, 400, 372, 237, 96 | |
| CR3a | 3097, 2291, 1875, 1505, 1334, 1239, 1208, 888, 635, 579, 420, 389, 301, 226, 76 | |
| TS1a | 3048, 1860, 1576, 1472, 1362, 1297, 1202, 984, 718, 586, 392, 285, 205, 144, 1041i | |
| TS1b | 3174, 3078, 1604, 1520, 1364, 1247, 1214, 1104, 512, 358, 213, 152, 96, 21, 1194i | |
| TS2a | 3044, 1858, 1555, 1480, 1324, 1285, 1109, 711, 697, 423, 349, 256, 256, 181, 108, 977i | |
| TS2b | 3133, 3052, 1807, 1553, 1335, 1237, 1120, 1001, 368, 320, 193, 123, 68, 29, 705i | |
| TS3a | 3044, 1864, 1578, 1488, 1283, 1265, 1058, 688, 604, 368, 300, 249, 161, 88, 757i | |
| TS3b | 3125, 3045, 1885, 1549, 1304, 1233, 1020, 936, 312, 248, 145, 95, 60, 7, 549i | |

[a] From [25]

[b] From [26]

[c] From [27]

## Energetics

Table 2 lists the reaction enthalpies $\left(\Delta H_{298}^0\right)$ and potential barrier heights ($\Delta E^{TS}$), including zero-point energy (ZPE) corrections, for the six reaction channels, calculated at the MC-QCISD//MP2/6-311+G(d,p) level. From Table 2, it is apparent that the six individual reaction channels are all exothermic, which is consistent with Hammond's postulate [24] discussed above.

Potential energy diagrams for the reactions NO + CH$_2$FO → products, NO + CH$_2$ClO → products, and NO + CH$_2$BrO → products, including ZPE corrections calculated at the MC-QCISD//MP2/6-311+G(d,p) level, are plotted in Figs. 2, 3, and 4, respectively. To facilitate comparisons, the energies of the reactants are set to zero. For the complexes CR1a, Cr2a, and CR3a, the energies were calculated to be −37.63, −49.43, and −53.08 kJ mol$^{-1}$, respectively, at the MC-QCISD//MP2/6-311+G(d,p) level. The energies of the complexes are close to those of the reactants, and it is unclear whether the complexes really do exist. According to the BSSE-corrected results obtained at the MP2/6-311+G(d,p) level, the relative energies of the complexes CR1a, Cr2a,

and CR3a are −100.94, −110.68, and −118.21 kJ mol$^{-1}$, respectively. The energies of these complexes are much lower than the reactants, which means that these weakly bonded complexes exist. For the six reaction channels, the potential barrier heights for the reaction channels R1a, R2a, and R3a are lower than those for R1b, R2b, and R3b by 169.02, 111.51, and 105.23 kJ mol$^{-1}$ when calculated at the MC-QCISD//MP2/6-311+G(d,p) level, respectively. At the same time, the reaction channels R1a, R2a, and R3a are more exothermic than R1b, R2b, and R3b by about 83.22, 30.43, and 11.51 kJ mol$^{-1}$, respectively. As a result, R1a, R2a, and R3a are more thermodynamically and kinetically favorable than R1b, R2b, and R3b, indicating that R1a, R2a, and R3a are the major reaction channels whereas paths R1b, R2b, and R3b are only very rarely used. Thus, we only calculated the rate constants for the three hydrogen abstraction reaction channels R1a, R2a, and R3a.

## Rate constants

Dual-level dynamics calculations [5–9] of R1a, R2a, and R3a were carried out at the MC-QCISD//MP2/6-311+G(d,p)

**Table 2** The reaction enthalpies at 298 K $\left(\Delta H_{298}^0\right)$ and the barrier heights ($\Delta E^{\mathrm{TS}}$) (kJ mol$^{-1}$) with zero-point energy (ZPE) corrections for the reactions of CH$_2$XO (X = F, Cl, Br) radicals with the NO radical, calculated at the MC-QCISD//MP2/6-311+G(d,p) level

| Parameter calculated | Reaction channel | MC-QCISD //MP2 |
|---|---|---|
| $\Delta H_{298}^0$ | NO + CH$_2$FO → CHFO + HNO (R1a) | −181.88 |
| | NO + CH$_2$FO → CH$_2$O + FNO (R1b) | −98.66 |
| | NO + CH$_2$ClO → CHClO + HNO (R2a) | −170.87 |
| | NO + CH$_2$ClO → CH$_2$O + ClNO (R2b) | −140.44 |
| | NO + CH$_2$BrO → CHBrO + HNO (R3a) | −166.72 |
| | NO + CH$_2$BrO → CH$_2$O + BrNO (R3b) | −155.21 |
| $\Delta E^{\mathrm{TS}}$+ZPE | NO + CH$_2$FO → CHFO + HNO (R1a) | −21.22 |
| | NO + CH$_2$FO → CH$_2$O + FNO (R1b) | 147.80 |
| | NO + CH$_2$ClO → CHClO + HNO (R2a) | −30.47 |
| | NO + CH$_2$ClO → CH$_2$O + ClNO (R2b) | 81.04 |
| | NO + CH$_2$BrO → CHBrO + HNO (R3a) | −32.06 |
| | NO + CH$_2$BrO → CH$_2$O + BrNO (R3b) | 73.17 |

level. The rate constants of the three hydrogen abstraction reaction channels, $k_{1a}$, $k_{2a}$, and $k_{3a}$, were evaluated by conventional transition state theory (TST), improved canonical variational transition state theory (ICVT), and ICVT with the small-curvature tunneling (SCT) correction in a wide temperature range (200–1,500 K). The ICVT/SCT rate constants $k_{1a}$, $k_{2a}$, and $k_{3a}$ are plotted against the reciprocal of temperature in Fig. 5 and are given in Table 3 along with experimental results [3]. The theoretically calculated rate constant values of $k_{2a}$ are in good agreement with these experimental values [3]. For example, the ratio $k_{\mathrm{ICVT/SCT}}$/ $k_{\mathrm{exptl}}$ is 1.25, 1.12, 0.96, and 0.88 at 265, 280, 289, and 306 K, respectively. The theoretical ICVT/SCT rate constant for the reaction channel NO + CH$_2$ClO → CHClO + HNO (R2a) is $2.32 \times 10^{-12}$ cm$^3$ molecule$^{-1}$ s$^{-1}$, which is lower than that ($4.09 \times 10^{-12}$ cm$^3$ molecule$^{-1}$ s$^{-1}$) for the reaction channel NO + CH$_2$FO → CHFO + HNO (R1a) but higher than



**Fig. 3** Potential energy surface for the reaction NO + CH$_2$ClO. Relative energies (kJ mol$^{-1}$) were calculated at the MC-QCISD//MP2/6-311+G(d,p) + ZPE level

that ($4.11 \times 10^{-13}$ cm$^3$ molecule$^{-1}$ s$^{-1}$) for the reaction channel NO + CH$_2$BrO → CHBrO + HNO (R3a) at 298 K. The theoretical activation energy ($E_a$) was estimated based on the calculated ICVT/SCT rate constants, and it was found that the corresponding $E_a$ value for reaction channel R2a (−5.40 kJ mol$^{-1}$) is higher than that for reaction channel R1a (7.24 kJ mol$^{-1}$) but lower than that for reaction channel R3a (−5.02 kJ mol$^{-1}$) in 350–600 K, which is in accord with its kinetic superiority. These results are consistent with the qualitative assessment based on potential energy barrier heights.

Because experimental knowledge of the title reactions is limited, we hope that our research into the kinetics of the title reactions may provide useful information for future laboratory investigations. In order to provide more convenient reference data for future experimental measurements, three-parameter fits of the ICVT/SCT rate constants for the three hydrogen abstraction reaction channels over the temperature range 200–1,500 K were performed, and the resulting expressions are given below (in units of cm$^3$ molecule$^{-1}$ s$^{-1}$):



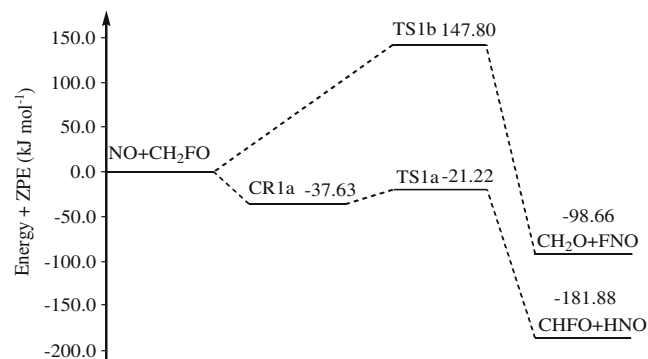**Fig. 2** Potential energy surface for the reaction NO + CH$_2$FO. Relative energies (in kJ mol$^{-1}$) were calculated at the MC-QCISD//MP2/6-311 +G(d,p) + ZPE level
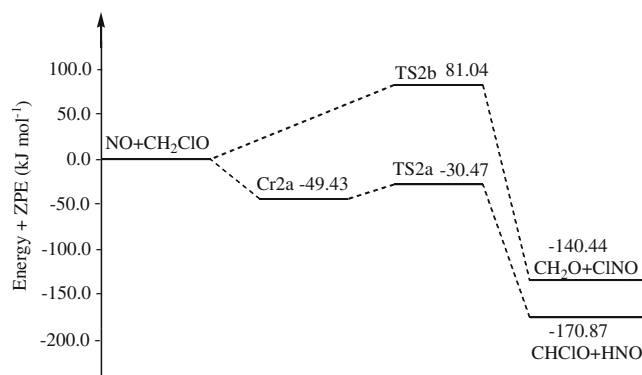


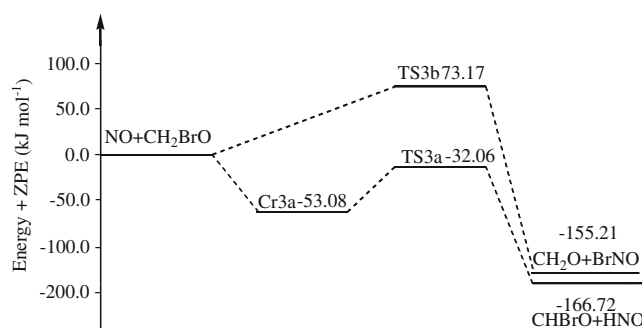**Fig. 4** Potential energy surface for the reaction NO + CH$_2$BrO. Relative energies (in kJ mol$^{-1}$) were calculated at the MC-QCISD//MP2/6-311+G(d,p) + ZPE level
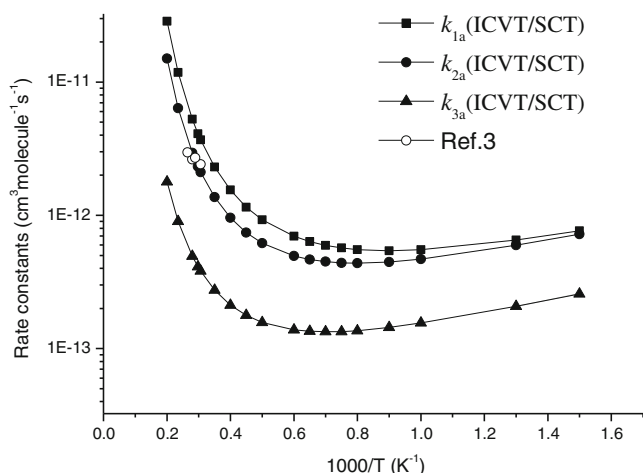
**Fig. 5** ICVT/SCT rate constants calculated at the MC-QCISD//MP2/6-311+G(d,p) level for the three hydrogen abstraction reaction channel rate constants $k_{1a}$, $k_{2a}$, and $k_{3a}$ (in $cm^3$ $molecule^{-1}$ $s^{-1}$) plotted against $1000/T$ (where $T$ is between 200 and 1,500 K)

$$k_{1a}(T) = 0.32 \times 10^{-18} T^{1.83} \exp(1748.54/T)$$
$$k_{2a}(T) = 0.22 \times 10^{-19} T^{2.19} \exp(1770.19/T)$$
$$k_{3a}(T) = 0.88 \times 10^{-20} T^{2.20} \exp(1513.82/T)$$

## Conclusions

In this work, the multi-channel reactions NO + $CH_2XO$ (X = F, Cl, Br) were investigated theoretically. Performing

calculations at the MP2/6-311+G(d,p) level, we obtained potential energy surface data, and the energies of the stationary points and a few extra points along the minimum energy path were refined at the MC-QCISD level. Six reaction channels were identified for the title reactions. By comparing barrier heights and performing a molecular electrostatic potential analysis, the hydrogen abstraction reaction channels were identified as the major pathways. The difference between the transition state energy and the corresponding complex energy for the reaction channel increases in the order R1a < R2a < R3a. The rate constants for the three major reaction channels were calculated by ICVT with the SCT correction at the MC-QCISD//MP2/6-311+G(d,p) level. The calculated results show that the values of the ICVT/SCT rate constants decrease as the size of the halogen atom increases, in the order $k_{1a}$(ICVT/SCT) > $k_{2a}$(ICVT/SCT) > $k_{3a}$(ICVT/SCT). The values of the ICVT/SCT rate constant $k_{2a}$ are in good agreement with the corresponding experimental values available. The three-parameter rate–temperature formulae for the three hydrogen abstraction reaction channels were fitted with the following expressions (in $cm^3$ $molecule^{-1}$ $s^{-1}$) in the temperature range 200–1,500 K:

$$k_{1a}(T) = 0.32 \times 10^{-18} T^{1.83} \exp(1748.54/T)$$

$$k_{2a}(T) = 0.22 \times 10^{-19} T^{2.19} \exp(1770.19/T)$$

$$k_{3a}(T) = 0.88 \times 10^{-20} T^{2.20} \exp(1513.82/T)$$

**Table 3** Calculated ICVT/SCT rate constants ($cm^3$ $molecule^{-1}$ $s^{-1}$) for reaction channels R1a, $k_{1a}$, R2a, $k_{2a}$, and R3a, $k_{3a}$ in the temperature range 200–1,500 K, as calculated at the MC-QCISD//MP2/6-311+G(d,p) level

| $T$ (K) | $k_{1a}$(ICVT/SCT) | $k_{2a}$(ICVT/SCT) | Experimental $k$ values from [3] | $k_{3a}$(ICVT/SCT) |
|---|---|---|---|---|
| 200.00 | $2.86 \times 10^{-11}$ | $1.50 \times 10^{-11}$ | | $1.78 \times 10^{-12}$ |
| 235.00 | $1.18 \times 10^{-11}$ | $6.36 \times 10^{-12}$ | | $9.01 \times 10^{-13}$ |
| 265.00 | $6.68 \times 10^{-12}$ | $3.69 \times 10^{-12}$ | $2.96 \times 10^{-12}$ | $5.87 \times 10^{-13}$ |
| 280.00 | $5.26 \times 10^{-12}$ | $2.94 \times 10^{-12}$ | $2.63 \times 10^{-12}$ | $4.93 \times 10^{-13}$ |
| 289.00 | $4.62 \times 10^{-12}$ | $2.60 \times 10^{-12}$ | $(2.7 \pm 0.4) \times 10^{-12}$ | $4.48 \times 10^{-13}$ |
| 298.00 | $4.09 \times 10^{-12}$ | $2.32 \times 10^{-12}$ | | $4.11 \times 10^{-13}$ |
| 306.00 | $3.69 \times 10^{-12}$ | $2.11 \times 10^{-12}$ | $2.41 \times 10^{-12}$ | $3.82 \times 10^{-13}$ |
| 350.00 | $2.30 \times 10^{-12}$ | $1.37 \times 10^{-12}$ | | $2.75 \times 10^{-13}$ |
| 400.00 | $1.55 \times 10^{-12}$ | $9.58 \times 10^{-13}$ | | $2.12 \times 10^{-13}$ |
| 450.00 | $1.15 \times 10^{-12}$ | $7.43 \times 10^{-13}$ | | $1.78 \times 10^{-13}$ |
| 500.00 | $9.27 \times 10^{-13}$ | $6.19 \times 10^{-13}$ | | $1.57 \times 10^{-13}$ |
| 600.00 | $6.96 \times 10^{-13}$ | $4.96 \times 10^{-13}$ | | $1.38 \times 10^{-13}$ |
| 650.00 | $6.35 \times 10^{-13}$ | $4.66 \times 10^{-13}$ | | $1.35 \times 10^{-13}$ |
| 700.00 | $5.95 \times 10^{-13}$ | $4.49 \times 10^{-13}$ | | $1.34 \times 10^{-13}$ |
| 750.00 | $5.69 \times 10^{-13}$ | $4.40 \times 10^{-13}$ | | $1.34 \times 10^{-13}$ |
| 800.00 | $5.53 \times 10^{-13}$ | $4.37 \times 10^{-13}$ | | $1.36 \times 10^{-13}$ |
| 900.00 | $5.42 \times 10^{-13}$ | $4.46 \times 10^{-13}$ | | $1.44 \times 10^{-13}$ |
| 1000.00 | $5.52 \times 10^{-13}$ | $4.69 \times 10^{-13}$ | | $1.56 \times 10^{-13}$ |
| 1300.00 | $6.53 \times 10^{-13}$ | $5.97 \times 10^{-13}$ | | $2.08 \times 10^{-13}$ |
| 1500.00 | $7.65 \times 10^{-13}$ | $7.21 \times 10^{-13}$ | | $2.57 \times 10^{-13}$ |

# References

1. Heeb NV, Dolezal IS, Buhrer T, Mattrel P, Wolfensberger M (1995) Chemosphere 31:3030
2. Tuazon EC, Atkinson R (1993) J Atmos Chem 17:179
3. Fuxiang W, Robert WC (2001) J Phys Chem 105:1423
4. McGivern WS, Kim H, Francisco JS, North SW (2004) J Phys Chem A 108:7247
5. Bell RL, Truong TN (1994) J Chem Phys 101:10442
6. Truong TN, Duncan WT, Bell RL (1996) In: Laird BB, Ross RB, Ziegler T (eds) Chemical applications of density functional theory. American Chemical Society, Washington, DC, p 85
7. Truhlar DG (1995) In: Heidrich D (ed) The reaction path in chemistry: current approaches and perspectives. Kluwer, Dordrecht, p 229
8. Corchado JC, Espinosa-Garcia J, Hu W-P, Rossi I, Truhlar DG (1995) J Phys Chem 99:687
9. Hu W-P, Truhlar DG (1996) J Am Chem Soc 118:860
10. Boys SF, Bernardi F (1970) Mol Phys 19:553
11. Fast PL, Truhlar DG (2000) J Phys Chem A 104:6111
12. Corchado JC, Chuang Y-Y, Fast PL, Hu W-P, Liu Y-P, Lynch GC, Nguyen KA, Jackels CF, Fernandez-Ramos A, Ellingson BA, Lynch BJ, Zheng JJ, Melissasa VS, Villa J, Rossi I, Coitino EL, Pu JZ, Albu TV, Steckler R, Garrett BC, Isaacson AD, Truhlar DG (2007) Polyrate, version 9.7. Department of Chemistry and Supercomputer Institute, University of Minnesota, Minneapolis
13. Truhlar DG, Garrett BC (1980) Acc Chem Res 13:440
14. Truhlar DG, Isaacson AD, Garrett BC (1985) In: Baer M (ed) The theory of chemical reaction dynamics, vol 4. CRC, Boca Raton, p 65
15. Frisch MJ, Head-Gordon M, Pople JA (1990) Chem Phys Lett 166:275
16. Frisch MJ, Head-Gordon M, Pople JA (1990) Chem Phys Lett 166:281
17. Handy NC, Schaefer HF III (1984) J Chem Phys 81:5031
18. Pople JA, Raghavachari K, Schlegel HB, Binkley JS (1979) Int J Quantum Chem Quantum Chem Symp S13:225
19. Frisch MJ, Trucks GW, Schlegel HB, Scuseria GE, Robb MA, Cheeseman JR, Montgomery JA Jr, Vreven T, Kudin KN, Burant JC, Millam JM, Iyengar SS, Tomasi J, Barone V, Mennucci B, Cossi M, Scalmani G, Rega N, Petersson GA, Nakatsuji H, Hada M, Ehara M, Toyota K, Fukuda R, Hasegawa J, Ishida M, Nakajima T, Honda Y, Kitao O, Nakai H, Klene M, Li X, Knox JE, Hratchian HP, Cross JB, Adamo C, Jaramillo J, Gomperts R, Stratmann RE, Yazyev O, Austin AJ, Cammi R, Pomelli C, Ochterski JW, Ayala PY, Morokuma K, Voth GA, Salvador P, Dannenberg JJ, Zakrzewski VG, Dapprich S, Daniels AD, Strain MC, Farkas O, Malick DK, Rabuck AD, Raghavachari K, Foresman JB, Ortiz JV, Cui Q, Baboul AG, Clifford S, Cioslowski J, Stefanov BB, Liu G, Liashenko A, Piskorz P, Komaromi I, Martin RL, Fox DJ, Keith T, Al-Laham MA, Peng CY, Nanayakkara A, Challacombe M, Gill PMW, Johnson B, Chen W, Wong MW, Gonzalez C, Pople JA (2003) Gaussian, Inc., Pittsburgh
20. Garrett BC, Truhlar DG (1980) J Phys Chem 84:805
21. Lu DH, Truong TN, Melissas VS, Lynch GC, Liu YP, Garrett BC, Steckler R, Issacson AD, Rai SN, Hancock GC, Lauderdale JG, Joseph T, Truhlar DG (1992) Comput Phys Commun 71:235
22. Lovas FJ, Tiemann E (1974) J Phys Chem Ref Data 3:609
23. Johnson RD III (ed) Computational Chemistry Comparison and Benchmark Database, NIST Standard Reference Database number 101 (August 2011 release). http://cccbdb.nist.gov/
24. Hammond GS (1955) J Am Chem Soc 77:334
25. Jacox ME, Milligan DE (1973) J Mol Spectrosc 48:536
26. Hisatsune IC, Heicklen J (1973) Can J Spectrosc 18:77
27. Shimanouchi T (2005) In: Linstrom PJ, Mallard WG (eds) NIST Chemistry WebBook, NIST Standard Reference Database number 69 (June 2005 release). http://webbook.nist.gov/chemistry/